

The Parkes Multibeam Pulsar Survey – II. Discovery and Timing of 120 Pulsars

D. J. Morris,¹ G. Hobbs,¹ A. G. Lyne,¹ I. H. Stairs,^{2,1} F. Camilo,³
 R. N. Manchester,⁴ A. Possenti,⁵ J. F. Bell,⁴ V. M. Kaspi,^{6,7} N. D’Amico,^{5,8}
 N. P. F. McKay,¹ F. Crawford^{6,9} and M. Kramer¹

¹ University of Manchester, Jodrell Bank Observatory, Macclesfield, Cheshire SK11 9DL

² National Radio Astronomy Observatory, PO Box 2, Green Bank, WV 24944, USA

³ Columbia Astrophysics Laboratory, Columbia University, 550 West 120th Street, New York, NY 10027, USA

⁴ Australia Telescope National Facility, CSIRO, PO Box 76, Epping NSW 1710, Australia

⁵ Osservatorio Astronomico di Bologna, via Ranzani 1, 40127 Bologna, Italy

⁶ Massachusetts Institute of Technology, Center for Space Research, 70 Vassar Street, Cambridge, MA 02139, USA

⁷ Physics Department, McGill University, 3600 University Street, Montreal, Quebec, H3A 2T8, Canada

⁸ Cagliari Astronomical Observatory, Loc. Poggio dei Pini, Strada 54, 09012 Capoterra (Ca), Italy

⁹ Department of Physics, Haverford College, Haverford, PA 19041, USA

2002 April 05

ABSTRACT

The Parkes multibeam pulsar survey is a sensitive survey of a strip of the Galactic plane with $|b| < 5^\circ$ and $260^\circ < l < 50^\circ$ at 1374 MHz. Here we report the discovery of 120 new pulsars and subsequent timing observations, primarily using the 76-m Lovell radio telescope at Jodrell Bank. The main features of the sample of 370 published pulsars discovered during the multibeam survey are described. Furthermore, we highlight two pulsars: PSR J1734–3333, a young pulsar with the second highest surface magnetic field strength among the known radio pulsars, $B_s = 5.4 \times 10^{13}$ G, and PSR J1830–1135, the second slowest radio pulsar known, with a 6-s period.

Key words: methods: observational — pulsars: general — pulsars: searches — pulsars: timing — pulsars: individual (PSR J1734–3333, PSR J1830–1135).

1 INTRODUCTION

The Parkes multibeam survey is an on-going survey of a 10° -wide strip along the Galactic plane ($|b| < 5^\circ$ and $l = 260^\circ$ to $l = 50^\circ$). The survey aims to detect a large sample of pulsars for population studies (more than 600 have been discovered so far) as well as find individual objects of interest including binary pulsars, young pulsars, EGRET source associations and high magnetic field pulsars. The survey uses a 13-beam receiver on the 64-m Parkes radio telescope, receiving two polarisations per beam over a 288-MHz bandwidth centred on 1374 MHz. The survey’s receiver system, data acquisition and control procedures, offline data analysis and calculations of sensitivity are published in Manchester et al. (2001) (hereafter Paper I) along with the discovery and timing parameters for 100 pulsars with declinations $< -35^\circ$. Timing observations of the majority of new pulsars with declinations $> -35^\circ$ are made using the Jodrell Bank 76-m Lovell radio telescope. Positional and rotational parameters for 120 high-declination pulsars are given in this paper along with corresponding derived parameters and averaged pulse pro-

files*. The parameters for a further 150 pulsars are given in Bell et al. (in preparation), hereafter Paper III.

In order to facilitate follow-up observations, it is desirable to determine a better position estimate than that available from the survey data. For this reason, a technique known as ‘gridding’ is carried out on newly discovered pulsars before long-term timing begins. This technique, introduced in Paper I, is described in detail here. We also describe the Jodrell Bank observing system, summarise some interesting properties of the sample of 370 pulsars published here and in Papers I and III, and highlight two pulsars: PSR J1734–3333, a young pulsar with a high surface magnetic field and PSR J1830–1135, a pulsar with a 6-s period.

2 TIMING OBSERVATIONS AND ANALYSIS

* The data release policy and results for the survey may be found at <http://www.atnf.csiro.au/research/pulsar/pmsurv>.

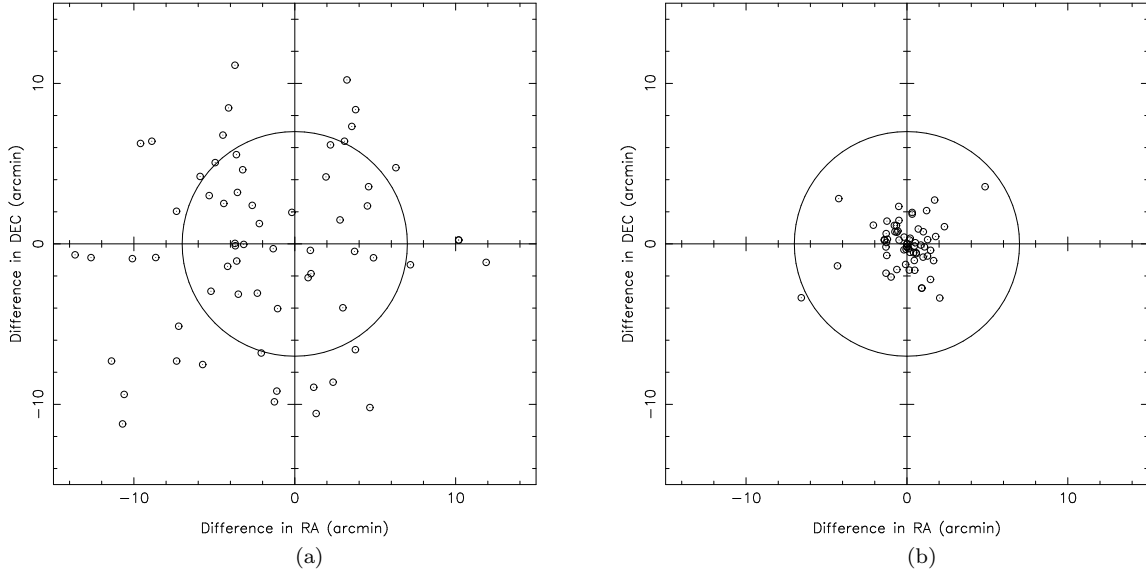


Figure 1. In (a) each point represents the offset between the initial candidate position and the precise position in right ascension (RA) and declination (DEC) resulting from one year of timing observations for the 82 pulsars published here and in Paper I that have been gridded; (b) shows the same for the positions given by the gridding observations. The circle represents the half-power beamwidth of the Parkes telescope.

2.1 Gridding

The centre of the discovery beam defines the initial position given to a pulsar candidate. If the pulsar is offset from the centre of the $14.^{\circ}4$ beam then it will be detected with a lower signal-to-noise ratio (S/N) than for an equivalent observation centred on the pulsar. Furthermore, if the pulsar is to be observed with the narrower beam of the Lovell telescope then the S/N may be further reduced, hence the most accurate position estimate available should be used until the precise position is determined from timing. The use of a more accurate position maximises the S/N and therefore reduces the amount of telescope time required to obtain a pulse arrival time. Improved knowledge of the position also reduces the density of observations required through the year to obtain a coherent solution without period ambiguities in the timing residuals.

In order to improve the position estimate, a ‘gridding procedure’ is carried out using the Parkes telescope. The original discovery position is re-observed (with a shorter integration time of a few minutes — the exact time depending on the S/N in the original discovery) along with four other integrations of similar durations at positions $9'$ to the North, South, East and West. The peak of a Gaussian beam shape (with a half-power width of $14.^{\circ}4$) fitted to the S/Ns in these consecutive observations determines the pulsar position with an uncertainty substantially smaller than a single beamwidth. Fig. 1a contains a scatter plot of the offset between the initial candidate position and the precise position determined after one year of timing observations for all of the pulsars with gridding observations (many of the earliest candidates were not ‘gridded’). Many pulsars lie outside the half-power beamwidth: the root-mean-square (rms) positional uncertainty is $7.^{\circ}2$. However, the rms positional error of $1.^{\circ}6$ for the differences between the gridded and precise positions (Fig. 1b) is well within the beamwidth, and the

typical area of uncertainty has been reduced by more than an order of magnitude.

2.2 Timing at Jodrell Bank

For most of the timing observations, we use the Lovell telescope at Jodrell Bank at a frequency near 1400 MHz. We employ a dual-channel cryogenic receiver system sensitive to the two hands of circular polarisation. Each hand of polarisation is down-converted, fed through a multichannel filterbank and digitized. Until August 1999, the filterbank consisted of $2 \times 32 \times 3$ MHz channels centred on 1376 MHz. Subsequent observations use a filterbank with $2 \times 64 \times 1$ MHz channels centred on 1396 MHz.

In the observing procedure, data are dedispersed and folded on-line according to the pulsar’s dispersion measure (DM) and topocentric period. The folded pulse profiles for each polarisation are stored for subsequent analysis. The duration of each observation is between 6 and 36 minutes (depending upon the flux of the pulsar) and is divided into a number of sub-integrations, each lasting between one and three minutes. During offline data processing, the polarisations are combined to produce the total intensity and the sub-integrations are added to produce a final averaged profile for the observation. Pulse times-of-arrival (TOAs) are determined by cross-correlating the profile with a template of high S/N. These TOAs are corrected to the solar system barycentre using the Jet Propulsion Laboratory DE200 solar-system ephemeris (Standish 1982). The positional and rotational parameters for the pulsar are then obtained by model-fitting the TOAs using TEMPO[†].

[†] See <http://pulsar.princeton.edu/tempo>.

Table 1. Positions, flux densities and pulse widths for 120 higher declination pulsars discovered in the Parkes multibeam pulsar survey. ‘A’ indicates pulsars that have been timed at Arecibo and ‘P’ denotes pulsars timed using the Parkes telescope. All other pulsars were timed using the Lovell telescope at Jodrell Bank. Radial angular distances are given in units of beam radii. PSRs J1841–0348, J1842–0415 and J1844–0310 were discovered independently by Lorimer et al. (2000).

PSR J	R.A. (J2000) (h m s)	Dec. (J2000) (° ' '')	<i>l</i> (°)	<i>b</i> (°)	Beam	Radial Dist.	<i>S/N</i>	<i>S</i> ₁₄₀₀ (mJy)	<i>W</i> ₅₀ (ms)	<i>W</i> ₁₀ (ms)
0729–1448	07:29:16.45(2)	−14:48:36.8(8)	230.39	1.42	12	0.27	49.1	0.7(1)	12.5	22
0737–2202	07:37:44.071(6)	−22:02:05.3(1)	237.69	−0.32	9	0.87	23.6	0.47(9)	6.3	20
1733–3322	17:33:55.21(8)	−33:22:03(4)	354.92	−0.24	1	0.63	61.2	0.8(2)	34.3	—
1734–3333 ^P	17:34:26.6(5)	−33:33:22(29)	354.81	−0.44	7	0.48	20.0	0.5(1)	164.1	—
1735–3258 ^P	17:35:56.9(3)	−32:58:19(19)	355.48	−0.38	5	0.92	10.1	0.46(9)	187.5	—
1737–3102	17:37:33.73(4)	−31:02:01(4)	357.30	0.37	9	0.57	39.8	0.6(1)	15.0	36
1737–3137	17:37:04.29(4)	−31:37:21(3)	356.74	0.14	10	1.23	20.2	0.8(2)	16.4	—
1738–2955 ^P	17:38:52.24(10)	−29:55:51(10)	358.38	0.72	2	0.89	16.2	0.29(6)	23.4	62
1739–3023	17:39:39.80(2)	−30:23:12(2)	358.09	0.34	1	0.66	49.1	1.0(2)	6.1	11
1739–3049	17:39:23.22(6)	−30:49:40(5)	357.68	0.15	4	0.86	17.6	0.5(1)	18.8	—
1739–3159	17:39:48.68(8)	−31:59:49(9)	356.74	−0.55	1	1.06	33.0	1.0(2)	53.5	—
1740–3052	17:40:50.031(5)	−30:52:04.1(3)	357.81	−0.13	7	1.19	26.1	0.7(2)	8.9	27
1741–2733	17:41:01.34(4)	−27:33:51(7)	0.64	1.58	3	0.61	77.2	1.1(2)	42.2	55
1741–2945	17:41:14.47(4)	−29:45:35(5)	358.80	0.38	12	0.36	15.9	0.6(1)	10.7	—
1741–3016	17:41:07.04(6)	−30:16:31(10)	358.35	0.13	6	1.26	38.7	2.3(5)	39.8	111
1743–3153	17:43:15.57(1)	−31:53:05(2)	357.22	−1.11	6	1.01	10.9	0.5(1)	11.3	—
1744–3130	17:44:05.68(1)	−31:30:04(3)	357.64	−1.06	12	0.41	62.1	0.7(1)	16.0	29
1747–2802 ^P	17:47:26.6(2)	−28:02:37(33)	0.97	0.12	6	1.03	10.2	0.5(1)	27.3	—
1749–2629	17:49:11.28(5)	−26:29:10(19)	2.50	0.59	7	0.35	52.6	0.7(2)	46.4	—
1750–2438	17:50:59.787(9)	−24:38:58(7)	4.29	1.19	13	0.90	41.2	0.5(1)	9.6	19
1751–2516 ^P	17:51:52.63(6)	−25:16:43(26)	3.85	0.69	1	0.72	7.0	0.22(4)	27.3	—
1752–2821	17:52:24.55(3)	−28:21:10(9)	1.27	−0.98	6	0.59	29.4	0.32(6)	11.5	20
1755–2521	17:55:59.71(9)	−25:21:27(48)	4.19	−0.19	7	1.49	17.3	0.7(2)	13.4	33
1755–2725	17:55:41.88(9)	−27:25:45(24)	2.43	−1.14	7	0.97	18.4	0.5(1)	23.8	—
1757–2223	17:57:50.772(4)	−22:23:49(4)	7.03	0.97	3	0.84	44.8	1.1(2)	2.3	5
1758–2206	17:58:44.45(3)	−22:06:45(19)	7.38	0.93	8	0.51	25.4	0.41(8)	16.6	—
1758–2540	17:58:31.94(9)	−25:40:49(46)	4.26	−0.81	6	0.62	35.1	0.65(1)	120.0	—
1758–2630 ^P	17:58:34.3(1)	−26:30:10(21)	3.55	−1.23	9	0.14	16.1	0.41(8)	15.6	—
1759–1940	17:59:57.04(2)	−19:40:29(5)	9.63	1.90	6	0.98	39.1	0.9(2)	19.6	—
1759–1956	17:59:35.42(4)	−19:56:08(15)	9.37	1.84	4	0.68	49.8	0.41(8)	37.9	—
1759–2302	17:59:49.23(9)	−23:02(3)	6.70	0.26	10	1.04	34.5	1.3(3)	61.5	—
1759–2307	17:59:30.95(2)	−23:07:17(46)	6.59	0.27	9	0.47	24.1	0.7(1)	22.4	52
1759–2549	17:59:35.12(9)	−25:49:07(34)	4.26	−1.08	5	1.30	11.6	0.6(1)	15.6	—
1801–1855	18:01:22.3(3)	−18:55:49(49)	10.45	1.98	12	0.52	26.2	0.47(9)	41.9	—
1801–1909	18:01:46.69(3)	−19:09:36(6)	10.30	1.78	9	0.97	26.6	0.5(1)	40.0	—
1802–1745	18:02:14.85(3)	−17:45:17(7)	11.57	2.38	10	0.57	19.5	0.21(4)	8.8	—
1802–2426	18:02:03.10(4)	−24:26:43(30)	5.73	−0.89	10	1.14	13.8	0.6(1)	22.2	—
1803–1857	18:03:59.06(3)	−18:57:19(8)	10.73	1.43	2	0.98	33.3	0.40(8)	25.6	43
1804–2228 ^P	18:04:28.19(9)	−22:28:18(55)	7.72	−0.40	5	0.04	10.1	0.20(4)	27.3	—
1805–2032	18:05:37.09(6)	−20:32:51(21)	9.53	0.31	2	0.81	21.4	0.7(1)	26.3	—
1805–2037	18:05:28.19(3)	−20:37:16(11)	9.45	0.31	5	1.16	10.6	0.34(7)	13.2	—
1806–1920	18:06:06.6(2)	−19:20:23(40)	10.63	0.80	11	1.14	15.6	1.9(4)	400.0	—
1806–2125	18:06:19.59(9)	−21:25:41(24)	8.86	−0.25	3	1.17	22.6	1.1(2)	26.4	55
1809–1429	18:09:45.510(8)	−14:29:25(1)	15.31	2.39	12	1.52	20.8	0.6(1)	11.0	27
1809–1917	18:09:43.147(6)	−19:17:38(1)	11.09	0.08	2	1.06	33.8	2.5(5)	18.0	26
1809–2004	18:09:15.9(2)	−20:04:12(57)	10.36	−0.20	10	0.35	24.2	0.9(2)	46.3	—
1810–1820	18:10:55.52(3)	−18:20:39(6)	12.06	0.29	5	0.78	19.0	0.7(2)	13.6	31
1810–2005	18:10:58.988(2)	−20:05:08.3(6)	10.54	−0.56	4	0.77	46.2	2.0(4)	7.2	11
1811–1736	18:11:55.01(1)	−17:36:36.9(13)	12.82	0.44	10	0.62	21.3	1.3(3)	23.4	63
1811–1835	18:11:29.72(9)	−18:35:44(13)	11.91	0.05	1	0.44	25.4	0.42(8)	16.7	—

Table 1. – *continued*

PSR J	R.A. (J2000) (h m s)	Dec. (J2000) (° ' '')	<i>l</i> (°)	<i>b</i> (°)	Beam	Radial Dist.	S/N	<i>S</i> ₁₄₀₀ (mJy)	<i>W</i> ₅₀ (ms)	<i>W</i> ₁₀ (ms)
1812–2102	18:12:20.93(6)	−21:02:36(15)	9.86	−1.30	12	0.61	58.3	1.4(3)	39.4	66
1813–2113	18:13:39.87(3)	−21:13:00(7)	9.85	−1.66	11	0.72	46.0	0.6(1)	13.1	—
1814–1649	18:14:37.35(4)	−16:49:28(5)	13.82	0.25	11	0.83	45.0	1.1(2)	28.0	58
1814–1744	18:14:43.0(2)	−17:44:33(33)	13.02	−0.21	1	1.40	22.1	0.7(1)	92.0	—
1815–1910	18:15:03.08(4)	−19:10:00(8)	11.81	−0.96	3	0.43	16.0	0.32(6)	25.4	52
1818–1519	18:18:14.6(3)	−15:19:43(36)	15.55	0.19	9	0.54	66.2	2.1(4)	130.4	—
1818–1541	18:18:37.52(3)	−15:41:45(5)	15.27	−0.06	8	0.88	26.2	1.0(2)	27.2	—
1819–1408	18:19:56.8(5)	−14:08:02(50)	16.80	0.39	5	0.19	27.4	0.5(1)	116.8	—
1819–1510	18:19:53.691(8)	−15:10:21(1)	15.88	−0.09	7	0.66	36.8	0.6(1)	6.9	—
1823–1347	18:23:24.25(8)	−13:47:54(9)	17.49	−0.19	4	1.01	14.5	0.41(8)	34.6	—
1823–1807 ^P	18:23:09.68(7)	−18:07:33(8)	13.64	−2.16	7	0.67	14.6	0.39(8)	34.6	—
1824–1159	18:24:56.15(1)	−11:59:53(1)	19.25	0.32	6	0.87	25.9	0.7(1)	10.8	—
1824–1423	18:24:57.387(7)	−14:23:05(1)	17.15	−0.80	4	0.92	49.0	0.8(2)	9.9	18
1826–1526	18:26:12.60(3)	−15:26:03(5)	16.36	−1.55	4	0.76	22.4	0.46(9)	13.4	—
1827–0934	18:27:45.88(2)	−09:34:16(1)	21.72	0.84	9	0.45	26.5	0.29(6)	19.5	—
1828–1101	18:28:18.859(9)	−11:01:50.9(8)	20.49	0.04	13	0.74	34.8	2.9(6)	9.9	49
1828–1336	18:28:42.85(4)	−13:36:45(5)	18.25	−1.24	6	0.62	36.5	0.26(5)	34.6	—
1830–1135	18:30:01.72(6)	−11:35:32(6)	20.19	−0.59	9	0.36	75.3	1.1(2)	62.2	171
1831–1223	18:31:12.8(1)	−12:23:31(11)	19.62	−1.22	10	0.30	77.5	1.2(2)	98.0	122
1831–1329	18:31:55.96(6)	−13:29:56(8)	18.72	−1.88	13	0.87	40.4	0.5(1)	47.1	82
1832–0644	18:32:42.67(5)	−06:44:02(3)	24.81	1.07	4	0.69	49.4	0.7(1)	27.3	—
1833–0559	18:33:07.60(5)	−05:59:25(5)	25.51	1.32	2	0.95	26.6	0.6(1)	41.4	—
1833–1055	18:33:58.40(3)	−10:55:31(3)	21.23	−1.14	6	0.76	38.4	0.5(1)	24.2	—
1834–0602	18:34:37.97(3)	−06:02:35(3)	25.64	0.96	12	0.54	34.2	0.8(2)	16.8	35
1835–0924	18:35:38.0(1)	−09:24:27(13)	22.77	−0.80	7	0.90	18.1	0.5(1)	41.6	—
1835–1020	18:35:57.55(1)	−10:20:05(1)	21.98	−1.30	12	0.58	123.3	1.9(4)	5.7	10
1837–0559	18:37:23.66(1)	−05:59:28.3(9)	26.00	0.38	9	0.85	18.8	0.5(1)	10.7	—
1837–0604	18:37:43.8(1)	−06:04:52(7)	25.96	0.26	11	0.80	17.7	0.7(2)	13.0	30
1837–1243	18:37:09.41(3)	−12:43:56(3)	19.98	−2.66	10	0.25	26.1	0.17(3)	24.4	—
1838–0453	18:38:11.19(6)	−04:53:23(3)	27.07	0.71	2	0.84	18.4	0.33(7)	12.7	—
1838–1046	18:38:26.48(4)	−10:46:57(4)	21.86	−2.05	2	1.49	14.3	0.5(1)	16.6	34
1839–0321	18:39:37.51(2)	−03:21:11(1)	28.60	1.09	6	0.55	15.7	0.27(5)	5.4	—
1839–0402	18:39:51.06(3)	−04:02:25(1)	28.02	0.73	5	0.83	23.0	0.21(4)	7.0	15
1839–0459	18:39:42.62(2)	−04:59:59(2)	27.15	0.32	7	0.86	19.8	0.30(6)	11.7	—
1839–06273	18:39:20.46(3)	−06:27:34(5)	25.81	−0.27	5	0.58	13.6	0.29(6)	23.2	—
1839–0643	18:39:09.80(1)	−06:43:45(1)	25.55	−0.35	1	1.10	42.6	1.4(3)	19.1	—
1841–0348	18:41:38.68(5)	−03:48:43(2)	28.42	0.44	1	0.51	74.3	1.4(3)	9.5	18
1842–0153	18:42:57.87(1)	−01:53:26.7(6)	30.28	1.02	8	0.83	28.0	0.6(1)	21.4	—
1842–0415	18:42:11.29(1)	−04:15:38.2(7)	28.09	0.11	3	0.66	32.8	0.36(7)	11.8	19
1843–0050	18:43:36.72(6)	−00:50:10(3)	31.30	1.36	5	0.99	15.7	0.24(5)	19.1	—
1843–0355	18:43:06.67(5)	−03:55:56(3)	28.48	0.06	2	0.65	16.4	0.8(2)	16.7	—
1843–0459	18:43:27.64(2)	−04:59:30(1)	27.58	−0.51	4	1.09	50.6	1.7(3)	56.0	76
1844–0310	18:44:45.48(5)	−03:10:37(2)	29.34	0.04	9	1.26	10.8	0.7(1)	20.4	—
1847–0438	18:47:37.93(1)	−04:38:15.3(9)	28.37	−1.27	5	0.83	53.8	0.5(1)	11.3	—
1847–0605	18:47:21.07(1)	−06:05:14.1(9)	27.05	−1.87	12	1.24	40.5	0.8(2)	13.1	38
1849+0127 ^A	18:49:44.2(2)	+01:27:23(4)	34.03	1.04	3	0.77	20.2	0.46(9)	17.0	—
1849–0317	18:49:57.85(3)	−03:17:31(3)	29.83	−1.17	12	0.20	61.8	0.7(1)	23.2	33
1850+0026	18:50:45.14(1)	+00:26:25.6(9)	33.25	0.35	6	0.97	50.0	1.0(2)	14.1	99
1852+0305 ^A	18:52:32.6(5)	+03:05:05(9)	35.80	1.16	7	1.26	11.2	0.8(2)	15.6	—
1853+0056 ^A	18:53:32.7(2)	+00:56:59(4)	34.02	−0.04	3	0.38	13.1	0.21(4)	5.4	—

Table 1. – *continued*

PSR J	R.A. (J2000) (h m s)	Dec. (J2000) (° ' ")	<i>l</i> (°)	<i>b</i> (°)	Beam	Radial Dist.	S/N	<i>S</i> ₁₄₀₀ (mJy)	<i>W</i> ₅₀ (ms)	<i>W</i> ₁₀ (ms)
1855+0422	18:55:41.4(1)	+04:22:47(4)	37.31	1.05	1	1.40	13.8	0.45(9)	42.7	—
1856+0404 ^A	18:56:26.6(3)	+04:04:26(5)	37.13	0.75	4	0.48	22.1	0.48(10)	6.6	—
1857+0210	18:57:40.90(4)	+02:10:58(3)	35.59	-0.39	7	0.90	15.1	0.30(6)	16.0	—
1858+0215	18:58:17.4(1)	+02:15:38(8)	35.72	-0.49	7	0.64	15.3	0.22(4)	32.5	—
1900+0227	19:00:38.60(4)	+02:27:32(2)	36.17	-0.92	5	1.10	20.0	0.33(7)	17.3	—
1901+0413 ^A	19:01:10.3(1)	+04:13:51(6)	37.81	-0.23	1	1.11	38.9	1.1(2)	83.5	—
1904+0412 ^{P, A}	19:04:31.382(4)	+04:12:05.9(1)	38.16	-0.99	10	0.16	13.4	0.23(5)	2.5	—
1905+0616	19:05:06.85(1)	+06:16:15.7(8)	40.07	-0.17	12	0.20	47.2	0.40(8)	9.3	20
1906+0912	19:06:28.46(3)	+09:12:57(1)	42.84	0.88	2	1.02	17.7	0.32(6)	16.7	—
1907+0740	19:07:44.12(1)	+07:40:22.6(9)	41.61	-0.10	7	1.04	29.5	0.41(8)	13.2	23
1907+0534 ^A	19:07:23.3(2)	+05:34:53(14)	39.72	-0.99	9	0.87	12.5	0.36(7)	8.9	—
1908+0909	19:08:07.44(1)	+09:09:12.4(5)	42.97	0.49	12	0.56	19.1	0.22(4)	6.9	—
1908+0839 ^A	19:08:18.51(4)	+08:39:59(1)	42.56	0.23	7	0.43	26.8	0.49(10)	5.1	—
1909+0912	19:09:19.91(5)	+09:12:54(2)	43.16	0.26	5	1.04	17.1	0.35(7)	10.0	—
1909+0616	19:09:51.21(4)	+06:16:52(2)	40.62	-1.21	2	0.32	14.8	0.33(7)	32.5	—
1910+0534	19:10:26.51(9)	+05:34:09(4)	40.06	-1.67	8	0.45	13.0	0.41(8)	25.8	—
1913+1145	19:13:43.88(6)	+11:45:33(1)	45.92	0.48	4	0.69	24.4	0.43(9)	14.4	—
1913+1011	19:13:20.341(3)	+10:11:22.97(7)	44.48	-0.17	9	0.53	19.0	0.5(1)	2.1	5
1913+0832 ^{P, A}	19:13:00.50(2)	+08:32:05.1(5)	42.98	-0.86	11	0.71	23.7	0.6(1)	77.0	—
1920+1110	19:20:13.31(6)	+11:10:59(3)	46.15	-1.20	8	0.73	16.2	0.39(8)	10.2	—

The search code produces an initial estimate of a pulsar's DM, and observations at Jodrell Bank use a hardware dedisperser giving an averaged pulse profile at a particular DM. In order to make a more precise measurement, we use either the discovery or the gridding observations that used the 288-MHz bandwidth available at Parkes. The band is divided into four sub-bands and the DM is obtained by fitting to the TOAs of the pulses determined from each sub-band.

The flux density scale at Jodrell Bank is calculated by switching a noise diode on and off between sub-integrations. The noise diode is calibrated using standard flux calibrators such as 3C295. The pulsar flux density for a single observation is then determined as the mean flux density in the profile averaged over the pulse period.

Included in this paper are ten pulsars with low flux densities and with declinations $> -35^\circ$ that were timed at the Parkes telescope because of the higher sensitivity afforded by the use of the larger bandwidth. The observing and data-reduction techniques used at Parkes are described in Paper I. A few pulsars were observed with both instruments, but for consistency, only Jodrell Bank data were used to produce the pulse profiles. Similarly, nine pulsars were timed on a monthly basis with the 305-m Arecibo telescope, using a $2 \times 128 \times 0.0625$ MHz filterbank centred on 1400 MHz. These pulsars were observed for 5-minute or shorter integrations, with the polarisations summed and the data folded on-line using the known DM and the predicted topocentric pulse period. TOAs were determined using a standard template as for the Jodrell Bank observations.

3 DISCOVERY AND TIMING OF 120 PULSARS

The two tables giving positional, discovery and flux parameters (Table 1) and rotational parameters (Table 2) take the same form as the equivalent tables in Paper I. In summary, Table 1 lists the positional properties of each pulsar: the pulsar's name, J2000 right ascension and declination from the timing solution and the corresponding Galactic coordinates. This table also contains discovery information: the beam in which the pulsar was detected, the radial angular distance of the pulsar from the beam centre and the S/N of the pulse profile in the discovery observation. The median flux density averaged over all the observations included in the timing solution and the pulse widths at 50 per cent and 10 per cent of the peak of the mean pulse profile are also included (the 10 per cent width is only measured for pulsars with high S/N).

Table 2 contains the solar-system barycentric pulse period P , period derivative \dot{P} , the epoch to which the period refers to, the number of TOAs used in the timing solution, the MJD range covered by the timing observations, the final rms value for the timing residuals and the pulsar's DM. A non-deterministic period second derivative has also been fitted to a few pulsars, indicated by asterisks in Table 2, which show significant amounts of timing noise.

Data sets for each pulsar have been folded at twice and three times the tabulated period in order to confirm that this represents the fundamental period for the pulsar. The TOAs range from October 1997 to March 2002 with the shortest data span being 1.0 years and the longest 4.2 years.

This paper includes data for four binary pulsars which have previously been published: PSRs J1740–3052 (Stairs et al. 2001), J1810–2005, J1904+0412 (Camilo et al. 2001) and J1811–1736 (Lyne et al. 2000). For completeness, their binary parameters are summarised in Table 3.

Table 2. Rotational parameters and dispersion measures for 120 pulsars discovered in the Parkes multibeam pulsar survey. Asterisks indicate those pulsars whose timing residuals contain significant timing noise which has been removed, to first order, by the fitting of a period double derivative.

PSR J	Period, P (s)	\dot{P} (10^{-15})	Epoch (MJD)	N_{TOA}	Data Span (MJD)	Residual (ms)	DM (cm^{-3} pc)
0729–1448*	0.251658714181(12)	113.2879(4)	51367.0	112	50758–51975	2.9	92.3(3)
0737–2202*	0.320366370453(3)	5.46883(9)	51581.0	163	50831–52199	0.8	95.7(4)
1733–3322	1.24591463402(8)	4.10(3)	51250.0	26	51026–51473	1.6	524.0(17)
1734–3333*	1.1690082980(19)	2278.97(4)	51457.0	34	51032–51881	19.0	578(9)
1735–3258	0.35096322944(12)	26.08(7)	51573.0	22	51393–51752	4.1	754(8)
1737–3102	0.76867227339(5)	37.334(6)	51112.0	31	50758–51464	2.0	280(6)
1737–3137*	0.45043237000(4)	138.756(2)	51234.0	53	50832–51517	2.5	488.2(10)
1738–2955*	0.4433980218(3)	81.861(4)	51528.0	20	51158–51898	0.8	223.4(6)
1739–3023*	0.11436793182(2)	11.40145(12)	51497.0	48	50727–52266	1.5	170.0(3)
1739–3049	0.239317178406(18)	2.1781(18)	51116.0	27	50758–51473	2.0	573(2)
1739–3159	0.87756123714(15)	0.197(15)	51158.0	20	50850–51464	3.1	337(5)
1740–3052	0.570309580513(16)	2.54969(4)	51452.0	139	51032–51872	0.8	740.9(2)
1741–2733	0.89295866978(6)	0.148(8)	51184.0	36	50904–51463	1.6	149.2(17)
1741–2945	0.223557828541(15)	0.634(2)	51088.0	31	50764–51410	1.9	310.3(12)
1741–3016	1.89374869377(18)	8.99(6)	50959.0	27	50728–51188	2.3	382(6)
1743–3153*	0.193105399932(6)	10.5674(3)	51309.0	40	50879–51737	0.9	505.7(12)
1744–3130	1.06606087128(4)	21.224(12)	50975.0	26	50760–51188	0.6	192.9(7)
1747–2802	2.7800791979(8)	2.37(12)	51312.0	20	51037–51586	6.2	835(14)
1749–2629	1.33538779057(13)	1.72(3)	51495.0	16	51251–51738	1.5	409(11)
1750–2438	0.712794036774(10)	10.797(3)	51491.0	26	51242–51738	0.3	476(5)
1751–2516*	0.39483578357(9)	2.644(2)	51383.0	22	51013–51752	1.8	556(3)
1752–2821	0.64022949952(4)	3.468(17)	50974.0	20	50761–51185	1.1	516.3(13)
1755–2521*	1.1759678772(3)	90.193(15)	51586.0	37	51243–51985	6.1	252(4)
1755–2725	0.26195467832(5)	0.014(9)	51492.0	21	51243–51739	3.4	115(5)
1757–2223	0.1853101015788(11)	0.7820(3)	51495.0	26	51250–51739	0.1	239.3(4)
1758–2206	0.430278250497(15)	0.956(4)	51495.0	22	51250–51740	0.8	678(4)
1758–2540	2.1072633712(4)	1.55(14)	50975.0	22	50762–51187	2.8	218.2(13)
1758–2630	1.20289346322(18)	5.17(8)	51244.0	15	51033–51454	2.2	328(3)
1759–1940	0.254720352269(7)	0.093(2)	51491.0	25	51242–51740	0.7	302.7(10)
1759–1956	2.8433888097(3)	18.57(5)	51495.0	22	51250–51740	1.5	236.4(19)
1759–2302	0.81071772906(12)	10.744(12)	51115.0	23	50767–51462	3.7	889.0(1)
1759–2307	0.55888867754(3)	3.762(3)	51110.0	36	50757–51462	1.1	812.6(15)
1759–2549	0.95654854873(11)	99.592(13)	51380.0	34	51021–51737	4.9	431(5)
1801–1855	2.5504982104(10)	0.2(3)	51495.0	15	51250–51740	6.0	484(14)
1801–1909	1.10872484960(5)	0.703(9)	51491.0	26	51242–51740	1.0	264(9)
1802–1745	0.51467137652(3)	0.564(11)	51719.0	24	51509–51929	0.9	264.2(3)
1802–2426	0.56900709018(3)	8.562(7)	51495.0	29	51250–51739	1.3	711(6)
1803–1857	2.86433773648(13)	15.17(4)	51491.0	24	51243–51739	1.2	392.0(11)
1804–2228	0.57051063348(10)	0.143(10)	51414.0	25	51087–51740	3.5	424(7)
1805–2032	0.40576948790(5)	8.394(7)	51149.0	19	50834–51462	2.5	932(2)
1805–2037	0.357806774953(13)	1.7555(16)	51388.0	30	51037–51739	1.5	708.1(16)
1806–1920*	0.8797908757(6)	0.02(2)	51271.0	28	50802–51739	13.5	683(7)
1806–2125*	0.48178844602(5)	117.295(14)	51063.0	37	50820–51305	3.5	750(3)
1809–1429	0.895285284345(13)	5.240(4)	51495.0	26	51250–51740	0.4	411.3(16)
1809–1917*	0.082746885745(2)	25.53546(3)	51506.0	50	50820–52191	0.5	197.1(4)
1809–2004	0.43481138633(16)	7.28(6)	51719.0	21	51509–51928	5.3	867.1(17)
1810–1820	0.153716278369(8)	0.052(3)	50972.0	35	50757–51186	1.1	452(3)
1810–2005	0.03282224432571(9)	0.000151(7)	51200.0	269	50757–51632	0.4	240.2(3)
1811–1736	0.104181954734(3)	0.0018(6)	51050.0	475	50801–51928	1.0	477(10)
1811–1835	0.5574636120(1)	6.315(13)	51184.0	22	50905–51463	2.2	761(11)

Table 2. – *continued*

PSR J	Period, P (s)	\dot{P} (10^{-15})	Epoch (MJD)	N_{TOA}	Data Span (MJD)	Residual (ms)	DM (cm^{-3} pc)
1812–2102	1.22335230807(9)	23.893(9)	51134.0	32	50802–51464	1.5	547.2(10)
1813–2113	0.426466240565(13)	2.081(6)	51018.0	29	50802–51233	0.6	462.3(15)
1814–1649	0.95746393536(7)	6.333(7)	51133.0	25	50801–51463	1.5	782(6)
1814–1744*	3.9758447335(15)	743.05(4)	51413.0	56	50850–51975	14.8	792(16)
1815–1910	1.24992353738(8)	36.30(3)	50954.0	23	50721–51186	1.4	547.8(4)
1818–1519	0.9396900396(5)	4.11(7)	51415.0	34	51091–51739	15.0	845(6)
1818–1541	0.55113377674(3)	9.676(7)	51491.0	25	51243–51739	1.4	690(5)
1819–1408	1.7884904528(16)	2.59(16)	51612.0	21	51295–51929	20.0	1075(41)
1819–1510	0.226538990075(4)	0.0079(9)	51492.0	25	51250–51733	0.4	421.7(11)
1823–1347	0.61710720555(12)	9.60(3)	51481.0	23	51250–51711	3.1	1044(6)
1823–1807	1.63679245172(17)	0.28(4)	51295.0	21	51036–51554	2.0	330(4)
1824–1159	0.362492078224(8)	5.379(2)	51495.0	28	51250–51739	0.6	463(2)
1824–1423	0.359394162457(6)	0.3923(19)	51719.0	27	51507–51929	0.3	428.3(11)
1826–1526	0.382072812116(17)	1.085(8)	51720.0	23	51509–51929	1.0	530(4)
1827–0934	0.512547817784(16)	7.227(4)	51491.0	27	51242–51740	0.7	259.2(5)
1828–1101*	0.072051632709(2)	14.80952(9)	51531.0	62	51088–51974	0.9	607.4(5)
1828–1336	0.86033211599(7)	0.995(15)	51495.0	24	51250–51740	1.9	494.7(18)
1830–1135*	6.2215526664(12)	47.75(4)	51563.0	34	51152–51974	3.9	257(6)
1831–1223	2.8579410013(6)	5.5(3)	51704.0	27	51477–51929	4.5	342(5)
1831–1329	2.1656793503(3)	2.99(6)	51494.0	21	51250–51737	2.6	338(5)
1832–0644	0.74429541939(5)	37.089(17)	51489.0	20	51250–51728	1.4	578(7)
1833–0559	0.48345888008(5)	12.35(3)	51719.0	21	51509–51928	2.0	353(6)
1833–1055	0.63364029817(3)	0.527(4)	51360.0	22	51088–51632	1.1	543(4)
1834–0602	0.48791359170(3)	1.828(10)	51704.0	25	51477–51929	1.3	445(4)
1835–0924	0.8591920352(3)	21.39(9)	51720.0	23	51509–51930	4.7	471(7)
1835–1020	0.302448108644(5)	5.9187(11)	51493.0	19	51250–51736	0.3	113.7(9)
1837–0559	0.201062574029(5)	3.3048(13)	51463.0	29	51186–51740	0.7	317.8(7)
1837–0604*	0.09629420774(3)	45.1724(8)	51749.0	73	51153–52344	11.5	462(1)
1837–1243	1.87601852435(11)	36.51(3)	51494.0	21	51250–51738	1.1	300(9)
1838–0453	0.38083077683(3)	115.660(8)	51493.0	24	51250–51735	1.8	621(9)
1838–1046	1.21835359632(8)	3.080(18)	51493.0	19	51250–51736	1.2	208(3)
1839–0321	0.238777817900(9)	12.520(3)	51489.0	24	51250–51728	0.8	449(2)
1839–0402	0.520939679547(17)	7.694(5)	51487.0	27	51250–51724	0.9	242(3)
1839–0459	0.58531903782(3)	3.308(5)	51426.0	23	51152–51699	1.1	243(3)
1839–06273	0.48491367908(4)	0.132(17)	51361.0	16	51153–51568	1.0	88.5(7)
1839–0643	0.449548149848(15)	3.638(7)	51368.0	20	51154–51581	0.5	497.9(16)
1841–0348	0.204068115056(17)	57.872(3)	51646.0	29	51359–51931	1.9	194.2(4)
1842–0153	1.05422825038(3)	6.722(4)	51432.0	27	51152–51710	0.7	434(5)
1842–0415	0.526682241575(12)	21.9366(12)	51589.0	31	51250–51928	0.8	194(6)
1843–0050	0.78259846861(8)	0.249(12)	51462.0	21	51184–51740	2.2	507(7)
1843–0355	0.132313618371(11)	1.040(3)	51490.0	28	51250–51729	2.0	798(3)
1843–0459	0.75496337007(3)	0.854(10)	51719.0	22	51507–51930	0.7	444.1(5)
1844–0310	0.52504914274(4)	10.235(4)	51593.9	53	51257–51931	3.3	836(7)
1847–0438	0.95799116473(3)	10.933(9)	51319.0	24	51092–51544	0.5	229(4)
1847–0605	0.778164353310(19)	4.645(7)	51719.0	23	51507–51930	0.5	207.9(18)
1849+0127	0.54215548135(9)	27.97(6)	51664.0	18	51478–51848	2.1	207(3)
1849–0317	0.66840782878(4)	22.030(18)	51720.0	21	51509–51931	1.1	42.9(28)
1850+0026	1.08184378189(3)	0.359(11)	51353.0	26	51140–51564	0.5	201.4(12)
1852+0305	1.3261485670(8)	0.1(6)	51664.0	18	51479–51848	6.2	320(12)
1853+0056	0.27557759958(6)	21.39(4)	51665.0	20	51480–51848	2.5	180.9(12)

Table 2. – *continued*

PSR J	Period, P (s)	\dot{P} (10^{-15})	Epoch (MJD)	N_{TOA}	Data Span (MJD)	Residual (ms)	DM (cm^{-3} pc)
1855+0422	1.6781063295(3)	0.93(9)	51446.0	22	51184–51707	4.1	438(6)
1856+0404	0.42025215518(9)	0.04(6)	51664.0	25	51479–51848	3.7	341.3(7)
1857+0210	0.63098305833(6)	14.03(2)	51721.0	22	51509–51931	1.6	783(11)
1858+0215	0.7458280320(3)	4.61(9)	51720.0	19	51509–51929	5.3	702.0(1)
1900+0227	0.37426157516(3)	5.705(12)	51721.0	25	51509–51931	1.5	201.1(17)
1901+0413	2.6630796830(8)	131.6(3)	51706.0	37	51479–51931	5.4	352(3)
1904+0412	0.0710948973807(3)	0.00011(3)	51450.0	65	51089–51804	0.2	185.9(7)
1905+0616	0.98970706304(3)	135.218(11)	51720.0	26	51507–51931	0.7	259(7)
1906+0912	0.77534458995(5)	0.132(19)	51360.0	19	51140–51579	1.0	265(5)
1907+0740	0.574697951954(17)	0.671(7)	51354.0	30	51138–51568	0.7	332(3)
1907+0534	1.1384027132(6)	3.15(12)	51719.0	24	51480–51957	10.5	524(4)
1908+0909*	0.336554651762(14)	34.8712(6)	51525.0	43	51138–51911	0.9	467.5(15)
1908+0839	0.185397243919(14)	2.3865(14)	51550.0	31	51251–51848	2.1	512(2)
1909+0912	0.222949273318(15)	35.805(5)	51496.0	27	51252–51740	1.8	421.5(17)
1909+0616	0.75599276085(18)	20.58(8)	51720.0	27	51508–51930	1.7	352(4)
1910+0534	0.45286735393(9)	1.92(4)	51709.0	24	51507–51909	3.2	484(3)
1913+1145	0.30606864497(3)	5.016(11)	51290.0	27	51094–51484	1.4	637(2)
1913+1011	0.03590861279827(15)	3.36768(6)	51697.0	88	51464–51929	0.2	178.8(3)
1913+0832*	0.134409003573(10)	4.5696(6)	51685.0	54	51223–52147	1.1	355.2(10)
1920+1110	0.50988582045(5)	0.156(19)	51719.0	15	51507–51929	1.6	182(3)

PSR J1837–0604, a young energetic pulsar, has been discussed in D’Amico et al. (2001) and between MJDs 51305 and 51894, a glitch occurred in PSR 1806–2125 with a magnitude ~ 2.5 times greater than any previously observed event (Hobbs et al. 2002).

For each pulsar, the profiles used in the determination of the TOAs for the timing analysis were averaged to form mean pulse profiles at 20 cm (Fig. 2). For each profile, the pulsar’s name, pulse period and DM are given along with the effective time resolution of the profile, and pulsars timed at Parkes or Arecibo are indicated. There are several small features in the baselines of some pulsar profiles which may be other pulse components or may be radio frequency interference; higher S/N observations are required to resolve this issue.

4 DISCUSSION

Table 4 lists derived parameters for the 120 pulsars. The first column contains the pulsar’s name, followed by \log_{10} of the characteristic age, $\tau_c = P/(2\dot{P})$ in years, the surface dipole magnetic field strength, $B_s = 3.2 \times 10^{19} (P\dot{P})^{1/2}$ in gauss and the rate of loss of rotational energy, $\dot{E} = 4\pi^2 I \dot{P} P^{-3}$ in erg s^{-1} , where a neutron star with moment of inertia $I = 10^{45} \text{ g cm}^2$ is assumed. The next two columns give the pulsar distance, d , computed from the DM assuming the Taylor & Cordes (1993) model for the Galactic distribution of free electrons, together with the corresponding Galactic z -height. The uncertainty in distance from this model is generally far greater than the precision with which the distance is quoted. The final column in Table 4 gives the radio luminosity $L_{1400} \equiv S_{1400} d^2$.

A P – \dot{P} diagram is shown in Fig. 3. The pulsars pub-

lished here and in Papers I and III are overlaid on previously known pulsars. Anomalous X-ray pulsars and soft γ -ray repeaters are included along with lines of constant surface magnetic field strength, a pulsar emission ‘death line’ and a theoretical boundary separating radio loud and radio quiet pulsars.

4.1 The sample of 370 pulsars

A full population analysis will follow the completion of the survey. Here, we briefly highlight some of the salient features of the sample of pulsars presented in this paper and in Papers I and III. To compare the Parkes multibeam pulsars with previously known pulsars, Paper I displayed histograms of period, DM and flux density. We continue this comparison with histograms of pulse widths, ages, magnetic fields and rate of loss of rotational energy for the 370 pulsars (Fig. 4). There is a clear similarity between the measured widths of the profiles of these pulsars and of previously known pulsars (Fig. 4a). The characteristic ages for our sample are lower than previously measured characteristic ages (Fig. 4b). The observed age difference likely arises because we search along the plane of the Galaxy, where pulsars are born and where older pulsars have drifted from. This is also indicated by the results of the Swinburne intermediate latitude survey which uses the same observing system and has discovered many intermediate age to old pulsars (Edwards et al. 2001). Lorimer et al. (1995) suggest that young pulsars have flatter radio spectra than older pulsars. Our high observing frequency may, therefore, be an additional reason for the discovery of so many young pulsars. However, this difference in spectral indices is not confirmed by Malofeev (1996) or Maron et al. (2000).

The possibility of a relationship between characteristic

Table 3. Binary pulsar parameters. Data are taken from Stairs et al. (2001) for J1740–3052, Camilo et al. (2001) for J1810–2005 and J1904+0412 and Lyne et al. (2000) for J1811–1736.

	J1740–3052	J1810–2005	J1811–1736	J1904+0412
Orbital period (d)	231.02965(3)	15.0120197(9)	18.779168(4)	14.934263(2)
Projected semi-major axis (s)	756.9087(4)	11.97791(8)	34.7830(8)	9.6348(1)
Eccentricity	0.5788720(4)	0.000025(13)	0.82802(2)	0.00022(2)
Longitude of periastron(deg)	178.64613(6)	...	127.661(2)	350(6)
Epoch of ascending node (MJD)	51353.51233(3)*	51198.92979(2)	51044.03702(3)*	51449.45(25)

* epoch of periastron

age and luminosity was also studied; the results are shown in Fig. 5a which is consistent with a constant radio luminosity for ages ~ 40 kyr–20 Myr, although there seems to be a significant reduction in luminosity for even older ages. The surface magnetic field histogram (Fig. 4c) displays two features: the lack of pulsars with low magnetic fields (reflecting the absence of millisecond and moderately recycled pulsars in our sample) and the relatively large number of high magnetic field pulsars, due to an excess of long period pulsars. A graph of surface magnetic field versus luminosity (Fig. 5b) is suggestive of the possibility that high magnetic field pulsars have a higher luminosity than their lower-field counterparts. A plot of 1400-MHz luminosity versus \dot{E} for our sample (Fig. 5c) shows no indication of any trend, however, these figures do not take any geometrical beaming effects into account.

The histogram of the rate of loss of rotational energy (Fig. 4d) contains a component representing highly energetic pulsars ($\dot{E} > 10^{36}$ erg s $^{-1}$). Three (PSRs J1809–1917, J1828–1101 and J1837–0604) are both young ($10^4 < \tau_c < 10^5$ yr) and energetic. PSR J1913+1011 is slightly older ($\tau_c = 170$ kyr), but has similar parameters to PSR B1951+32 in the supernova remnant CTB 80. These ‘Vela-like’ pulsars are discussed in Paper III.

The average pulse profiles (Fig. 2) are diverse: the majority contain a single component, $\sim 20\%$ contain multiple components and three (PSRs J1806–1920, J1828–1101 and J1913+0832) clearly have interpulses. Eight (PSRs J1734–3333, J1735–3258, J1809–2004, J1811–1736, J1818–1541, J1828–1101, J1833–0559 and J1837–0604) have features suggestive of scattering tails. Although in general pulsars showing evidence of scattering also have high DM, we find no simple relationship between DM and the width of the scattering tail (see Paper I).

4.2 PSR J1734–3333

Camilo et al. (2000) discuss PSR J1814–1744, whose inferred surface magnetic field strength, $B_s = 5.5 \times 10^{13}$ G, is the largest of any known radio pulsar. PSR J1734–3333 has a similar field strength of 5.2×10^{13} G (and has a very small age, $\tau_c = 8$ kyr). Both these values were calculated using the standard expression[‡] $B_s = 3.2 \times 10^{19} (P\dot{P})^{1/2}$ G. Taking these fields at face value, these pulsars thus have surface

[‡] Note that occasionally in the literature the magnetic field is calculated with an additional factor of two. In that case the field represents the maximum surface dipole field, as opposed to the value at the equator.

magnetic field strengths that are larger than the ‘quantum critical field’, $B_c = 4.4 \times 10^{13}$ G, at which the cyclotron energy equals the electron rest-mass energy. Baring & Harding (2001) propose that photon splitting may inhibit pair creation at these high magnetic fields and therefore hypothesize the existence of a boundary separating radio-loud and radio-quiet pulsars. This boundary is indicated on Fig. 3 assuming that the emission occurs from the surface of the neutron star and that the photons propagate parallel to the local field. PSRs J1734–3333 and J1814–1744 lie in the predicted radio quiescence region. However, as detailed in Baring & Harding (2001) the boundary moves up the P – \dot{P} diagram for emission away from the neutron star’s surface. For an emission radius of 1.5 times the neutron star’s radius, the boundary lies above all the known radio pulsars. We note that given the trend toward pulse narrowing with increasing spin period (Gould 1994), the fact that no radio counterparts of AXPs, which also lie above this boundary, have been detected, may be due to their radio beams not intersecting our line of sight (Gaensler et al. 2001).

The success of this survey at finding new pulsars with fields close to and above the critical field will help improve our understanding of the delineation between radio-loud and radio-quiet pulsars.

4.3 PSR J1830–1135

After the discovery of PSR J2144–3933, a radio pulsar with an 8.5-s period (Young, Manchester & Johnston 1999), there has been much interest in detecting long-period pulsars. PSR J1830–1135, with a period of 6-s, is the second slowest known radio pulsar. It lies on the P – \dot{P} diagram at the extreme right-hand edge of the ‘normal’ pulsars, but due to a relatively high surface magnetic field of $\sim 10^{13}$ Gauss, lies well above the ‘death line’ (Fig. 3). Although the magnetic field is below the critical field, PSR J1830–1135 (and PSR J1814–1744) lies roughly in the neighbourhood of some AXPs (shown as open crosses in Fig. 3). Pivovaroff, Kaspi & Camilo (2000) infer, using PSR J1814–1744, that the X-ray emission from AXPs depends upon more than the implied surface magnetic field strength. The reasons for this are, however, not well understood.

Among the 370 published Parkes multibeam pulsars, only PSR J1830–1135 has a period greater than 6 seconds. Although the search software limits candidates to periods below 5 seconds (see Paper I), strong long-period pulsars with narrow pulse profiles, such as PSR J1830–1135, may be detected from their second or third harmonics. The probability of detecting a pulsar is also dependent upon the width

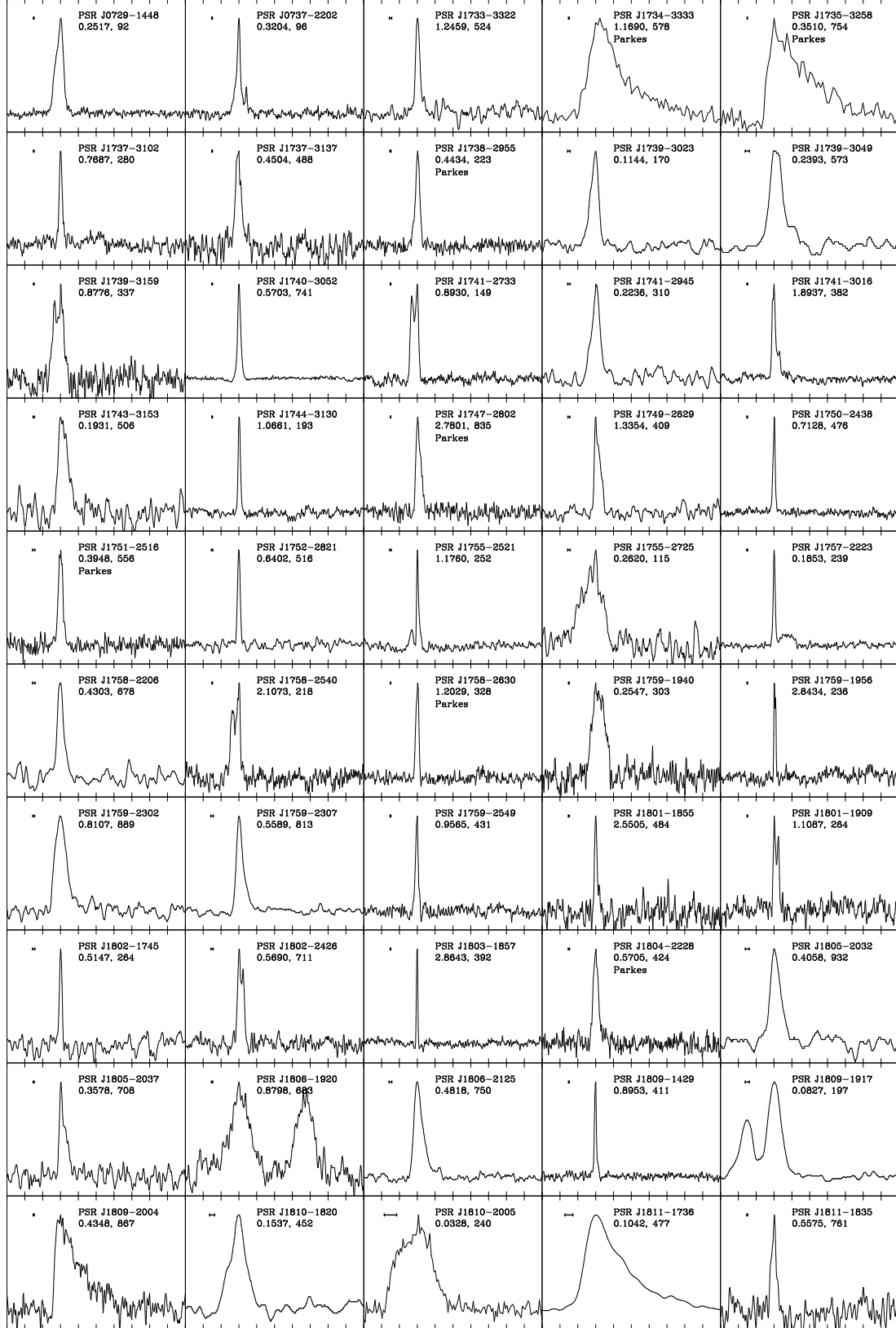


Figure 2. Mean pulse profiles for 120 pulsars discovered in the Parkes multibeam survey. The highest point in the profile is placed at phase 0.3. For each profile, the pulsar's name, pulse period (s) and DM (cm⁻³ pc) are given. The small horizontal bar to the left of the pulse indicates the effective time resolution of the profile, including the effects of interstellar dispersion.

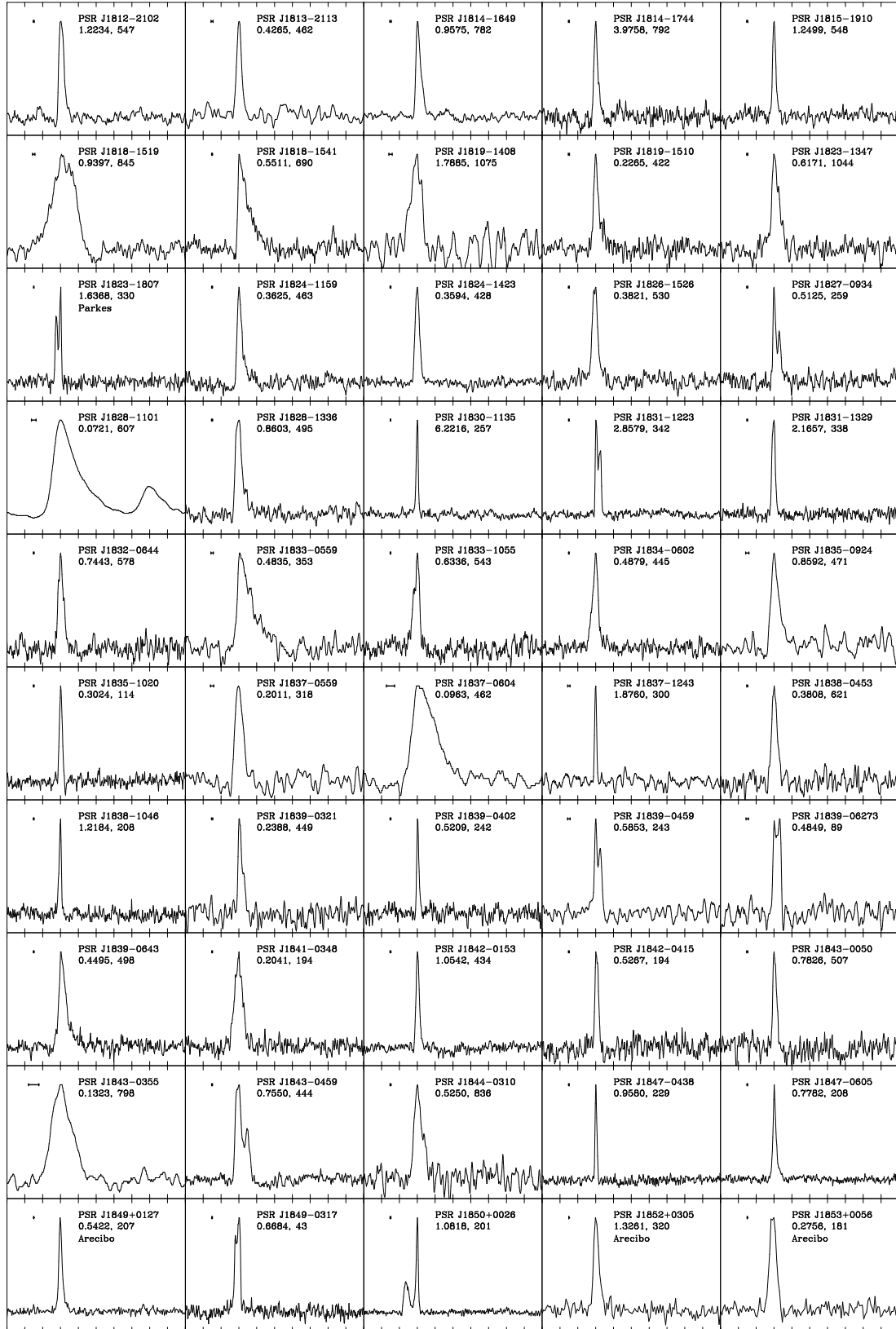


Figure 2. – continued

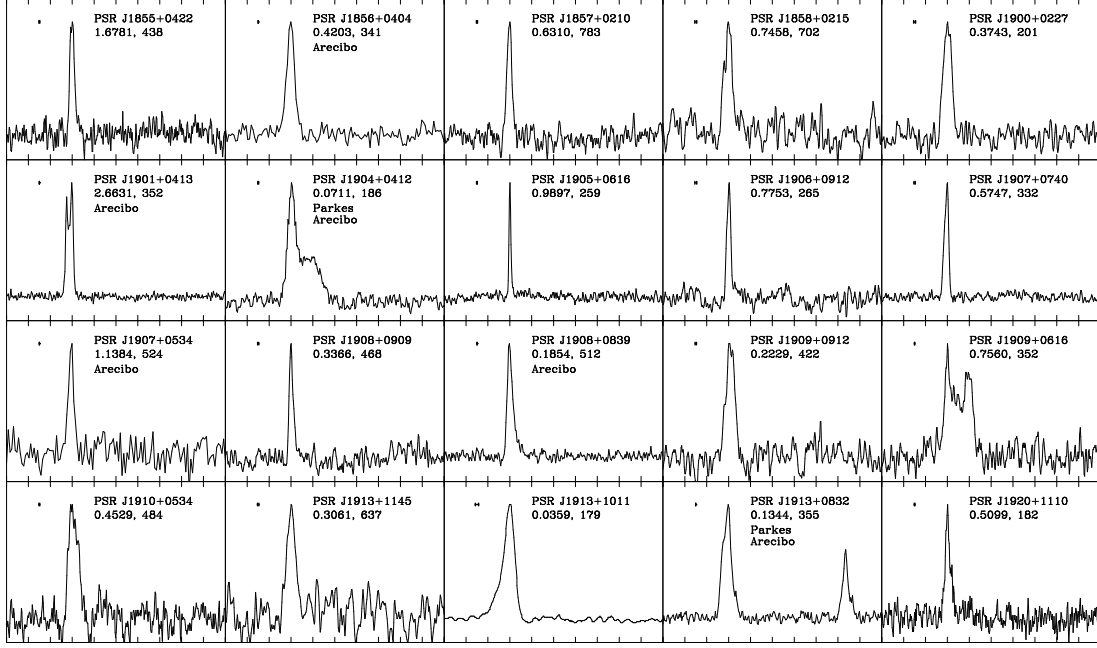
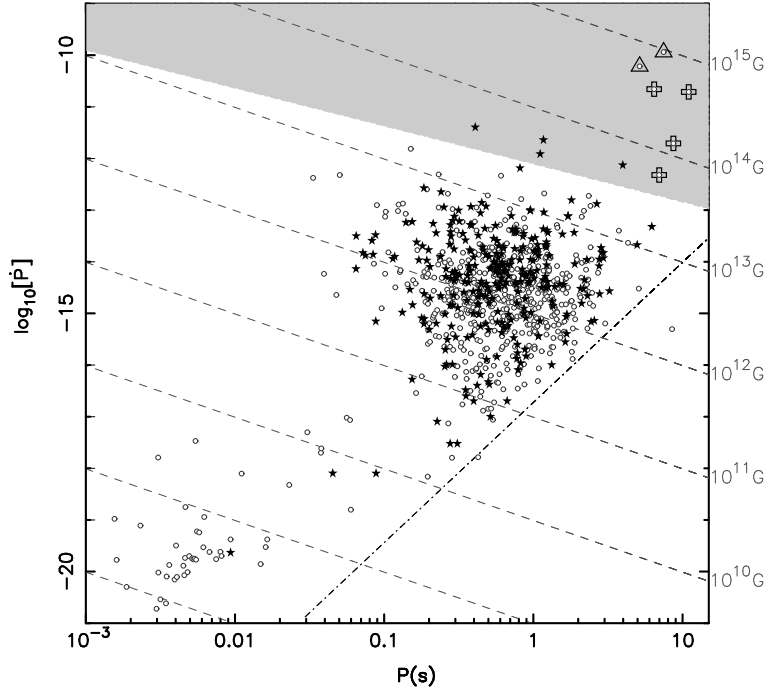
**Figure 2.** – *continued*

Figure 3. $P-\dot{P}$ diagram for the 370 pulsars published in this paper and in Papers I and III (stars) overlaid on previously known pulsars. Lines of constant magnetic field are shown as dashed lines. PSRs J1119–6217, J1726–3530, J1814–1744 (Camilo et al. 2000) and J1734–3333 lie above the theoretical boundary between radio-loud and radio-quiet pulsars (shown as the light shaded region). The boundary of this region is given by equation 10 in Baring & Harding (2001). Some of these pulsars are also close to the anomalous X-ray pulsars (AXPs), indicated as open crosses and the soft γ -ray repeaters (SGRs) shown as triangles. The placement of the AXPs and SGRs on this diagram assumes that they are spinning down due to magnetic dipole radiation in a manner similar to the radio pulsars. The ‘death line’ (dot-dashed line) is defined by $7 \log B_s - 13 \log P = 78$ (Chen & Ruderman 1993).

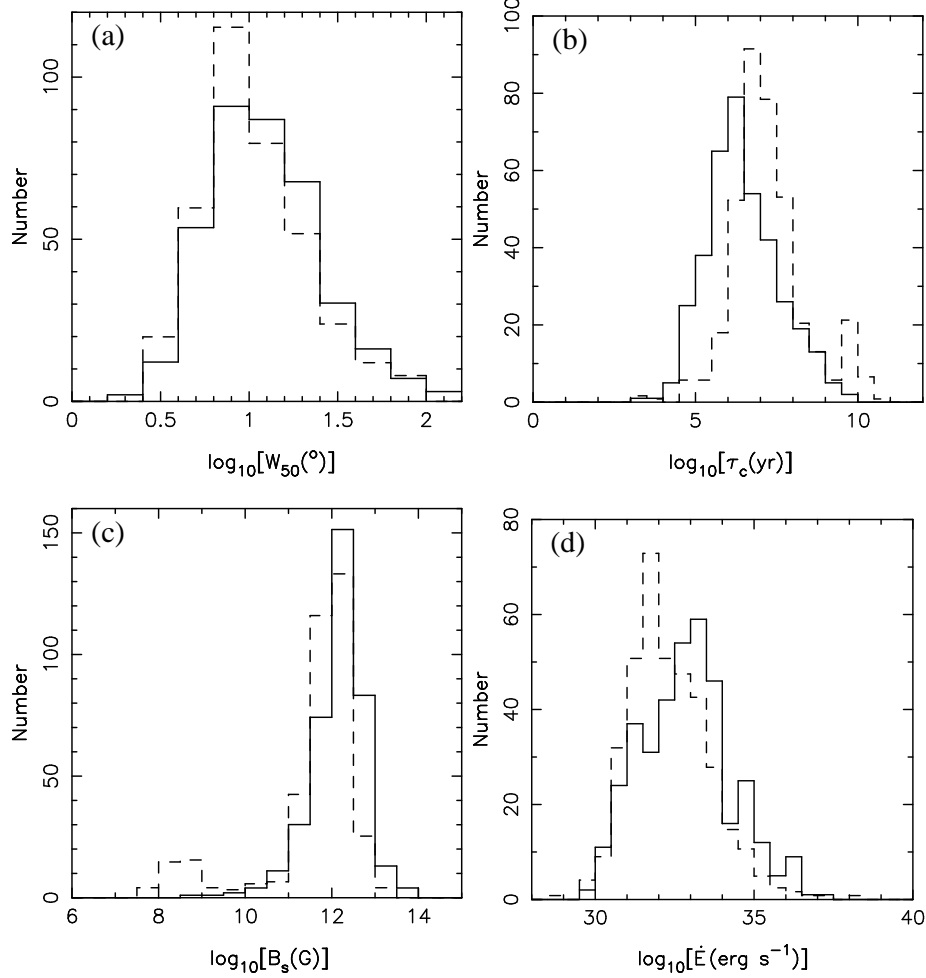


Figure 4. (a) Distribution in pulse width at 50% peak height for 370 multibeam pulsars (solid line) and for previously known pulsars (dashed line). For the latter, the vertical scale has been adjusted to equalise the number of pulsars in the two distributions. Panels (b), (c) and (d) similarly display distributions of characteristic age, surface magnetic field strength and rate of energy loss respectively.

of the pulsar beam, which decreases with increasing period (e.g. Rankin 1983 and Gould 1994). Although determination of the physical beam size requires polarisation information, the small angular pulse width of $\sim 4^\circ$ for PSR J1830–1135 is compatible with current understanding.

4.4 Conclusion

The sample of 370 pulsars reported here and in Papers I and III represents approximately half of the total number of new pulsars that we expect to discover on completion of this survey. Details of the remaining pulsars will be published in due course as the data from the timing observations become available. Once complete, the survey will provide a large and relatively unbiased dataset which may be used to study many aspects of pulsar physics.

ACKNOWLEDGEMENTS

We gratefully acknowledge the technical assistance provided by George Loone, Tim Ikin, Mike Kesteven, Mark Leach and the staff at the Parkes and Jodrell Bank Observatories toward the development of the Parkes multibeam pulsar system. We thank R. Bhat, D. Lorimer, M. McLaughlin and P. Freire for assistance with observations. DJM and GH acknowledge the receipt of post-graduate studentships from the UK Particle Physics and Astronomy Research Council. IHS received support from NSERC and Jansky postdoctoral fellowships. FC is supported by NASA grants NAG 5-9095 and NAG 5-9950. VMK is an Alfred P. Sloan Research Fellow and was supported in part by a US National Science Foundation (NSF) Career Award (AST-9875897) and by a Natural Sciences and Engineering Research Council of Canada grant (RGPIN 228738-00). The Parkes radio telescope is part of the Australia Telescope which is funded by the Commonwealth of Australia for operation as a National Facility managed by CSIRO. The Arecibo Observatory is part of the National Astronomy and Ionosphere Cen-

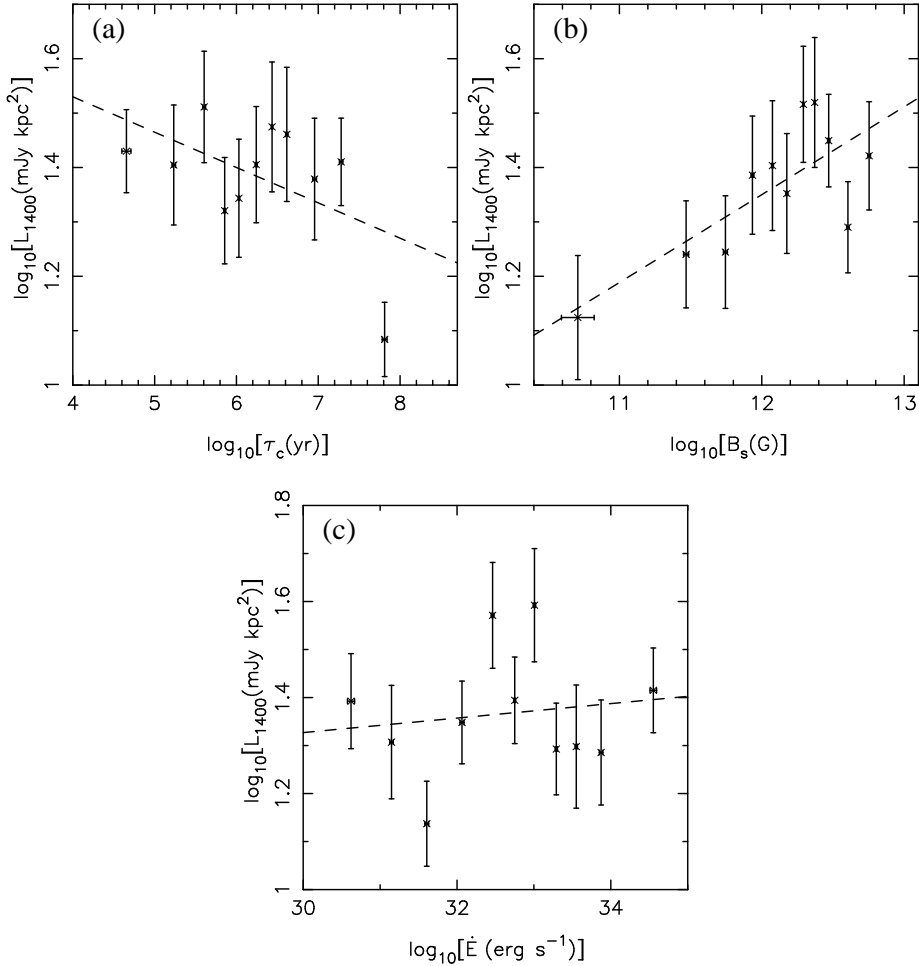


Figure 5. (a) Radio luminosity versus characteristic age ($\propto P\dot{P}^{-1}$), (b) luminosity versus surface magnetic field strength ($\propto [P\dot{P}]^{1/2}$) and (c) luminosity versus rate of loss of rotational energy ($\propto \dot{P}P^{-3}$) for 330 pulsars. Each point represents the average of 30 pulsars binned along the horizontal axis. The error bars for each point reflect the statistical scatter within each bin of 30 pulsars, and do not include other errors such as that due to the distance model uncertainty. The dashed lines represent a straight line fit to the data with a gradient of (-0.06 ± 0.04) for (a), (0.16 ± 0.05) for (b) and (0.02 ± 0.04) for (c).

ter, which is operated by Cornell University under a cooperative agreement with the US NSF.

REFERENCES

- Baring M. G., Harding A. K., 2001, ApJ, 547, 929
 Camilo F., Kaspi V. M., Lyne A. G., Manchester R. N., Bell J. F., D'Amico N., McKay N. P. F., Crawford F., 2000, ApJ, 541, 367
 Camilo F. et al., 2001, ApJ, 548, L187
 Chen K., Ruderman M., 1993, ApJ, 402, 264
 D'Amico N. et al., 2001, ApJ, 552, L45
 Edwards R. T., Bailes M., van Straten W., Britton M. C., 2001, MNRAS, 326, 358
 Gaensler B. M., Slane P. O., Gotthelf E. V., Vasisht G., 2001, ApJ, 559, 963
 Gould D. M., 1994, PhD thesis, The University of Manchester
 Hobbs G. et al., 2002, MNRAS, Submitted
 Lorimer D. R., Yates J. A., Lyne A. G., Gould D. M., 1995, MNRAS, 273, 411
 Lorimer D. R., Kramer M., Müller P., Wex N., Jessner A., Lange C., Wielebinski R., 2000, A&A, 358, 169
 Lyne A. G. et al., 2000, MNRAS, 312, 698
 Malofeev V., 1996, in Johnston S., Walker M. A., Bailes M., eds, Pulsars: Problems and Progress, IAU Colloquium 160. Astronomical Society of the Pacific, San Francisco, p. 271
 Manchester R. N. et al., 2001, MNRAS, 328, 17
 Maron O., Kijak J., Kramer M., Wielebinski R., 2000, A&AS, 147, 195
 Pivovaroff M., Kaspi V. M., Camilo F., 2000, ApJ, 535, 379
 Rankin J. M., 1983, ApJ, 274, 359
 Stairs I. H. et al., 2001, MNRAS, 325, 979
 Standish E. M., 1982, A&A, 114, 297
 Taylor J. H., Cordes J. M., 1993, ApJ, 411, 674
 Young M. D., Manchester R. N., Johnston S., 1999, Nature, 400, 848

Table 4. Derived parameters for 120 newly discovered pulsars. For pulsars in which the measured \dot{P} is not significant, only limits are given for τ_c , B_s and \dot{E} .

PSR J	$\log[\tau_c \text{ (yr)}]$	$\log[B_s \text{ (G)}]$	$\log[\dot{E} \text{ (erg s}^{-1}\text{)}]$	d (kpc)	z (kpc)	Luminosity (mJy kpc 2)
0729–1448	4.55	12.73	35.45	4.3	0.11	12.0
0737–2202	5.97	12.13	33.82	4.2	−0.02	8.3
1733–3322	6.68	12.36	31.92	6.3	−0.03	31.4
1734–3333	3.91	13.72	34.75	7.5	−0.06	29.3
1735–3258	5.33	12.49	34.38	11.1	−0.07	56.7
1737–3102	5.51	12.73	33.51	4.3	0.03	11.5
1737–3137	4.71	12.90	34.78	5.8	0.01	26.2
1738–2955	4.93	12.79	34.57	3.9	0.05	4.4
1739–3023	5.20	12.06	35.48	3.4	0.02	11.7
1739–3049	6.24	11.86	33.80	7.0	0.02	26.5
1739–3159	7.85	11.62	31.08	5.0	−0.05	24.0
1740–3052	5.55	12.59	33.73	10.8	−0.03	81.6
1741–2733	7.98	11.56	30.91	3.3	0.09	12.0
1741–2945	6.75	11.58	33.34	4.7	0.03	12.8
1741–3016	6.52	12.62	31.72	5.1	0.01	58.5
1743–3153	5.46	12.16	34.76	8.0	−0.15	32.0
1744–3130	5.90	12.68	32.84	3.7	−0.07	9.7
1747–2802	7.27	12.41	30.63	11.4	0.02	65.0
1749–2629	7.09	12.18	31.45	5.4	0.05	21.3
1750–2438	6.02	12.45	33.08	7.2	0.15	27.0
1751–2516	6.37	12.01	33.23	7.5	0.09	12.4
1752–2821	6.47	12.18	32.72	7.5	−0.13	18.0
1755–2521	5.31	13.02	33.34	4.2	−0.01	13.1
1755–2725	>8.48	<10.78	<31.48	2.8	−0.06	4.3
1757–2223	6.57	11.59	33.69	4.1	0.07	19.0
1758–2206	6.85	11.81	32.67	11.5	0.19	54.2
1758–2540	7.33	12.26	30.82	3.7	−0.05	8.9
1758–2630	6.57	12.40	32.08	5.0	−0.11	10.2
1759–1940	7.64	11.19	32.34	5.2	0.17	26.0
1759–1956	6.38	12.87	31.51	4.0	0.14	6.6
1759–2302	6.08	12.48	32.90	11.8	0.05	185.2
1759–2307	6.37	12.17	32.93	11.2	0.05	84.0
1759–2549	5.18	12.99	33.65	5.9	−0.11	20.9
1801–1855	>7.91	<12.06	<30.88	11.2	0.41	59.0
1801–1909	7.40	11.95	31.30	4.9	0.15	12.5
1802–1745	7.16	11.74	32.20	5.2	0.22	5.7
1802–2426	6.02	12.35	33.26	12.2	−0.19	90.8
1803–1857	6.48	12.82	31.40	6.2	0.15	15.4
1804–2228	7.80	11.46	31.48	5.3	−0.04	5.6
1805–2032	5.88	12.27	33.70	11.8	0.06	98.9
1805–2037	6.51	11.90	33.18	9.3	0.05	29.4
1806–1920	>8.45	<11.33	<30.46	10.4	0.14	204.4
1806–2125	4.81	12.88	34.61	9.9	−0.04	105.9
1809–1429	6.43	12.34	32.46	11.7	0.50	86.2
1809–1917	4.71	12.17	36.26	3.7	0.01	34.6
1809–2004	5.98	12.26	33.54	10.9	−0.04	104.6
1810–1820	7.67	10.96	32.76	5.6	0.03	22.9
1810–2005	9.60	9.32	32.18	4.0	−0.04	31.4
1811–1736	9.21	10.02	31.56	5.9	0.05	44.9
1811–1835	6.15	12.28	33.15	9.5	0.01	37.9

Table 4. – *continued*

PSR J	$\log[\tau_c \text{ (yr)}]$	$\log[B_s \text{ (G)}]$	$\log[\dot{E} \text{ (erg s}^{-1}\text{)}]$	d (kpc)	z (kpc)	Luminosity (mJy kpc 2)
1812–2102	5.91	12.74	32.72	9.5	−0.22	130.0
1813–2113	6.51	11.98	33.04	8.7	−0.25	47.7
1814–1649	6.38	12.40	32.45	9.6	0.04	101.4
1814–1744	4.93	13.74	32.67	10.2	−0.04	73.9
1815–1910	5.74	12.83	32.86	8.3	−0.13	22.0
1818–1519	6.56	12.30	32.30	10.0	0.03	208.0
1818–1541	5.96	12.37	33.36	8.3	−0.01	70.3
1819–1408	7.04	12.34	31.26	12.5	0.09	79.7
1819–1510	8.66	10.63	31.43	5.6	−0.01	19.4
1823–1347	6.01	12.39	33.20	11.1	−0.04	50.5
1823–1807	7.97	11.83	30.40	6.4	−0.25	16.0
1824–1159	6.03	12.15	33.65	6.1	0.03	26.8
1824–1423	7.16	11.58	32.52	6.1	−0.08	31.3
1826–1526	6.75	11.81	32.89	10.9	−0.29	54.7
1827–0934	6.05	12.29	33.32	4.5	0.07	5.9
1828–1101	4.89	12.02	36.20	7.2	0.01	149.8
1828–1336	7.14	11.97	31.79	7.8	−0.17	37.7
1830–1135	6.31	13.24	30.89	4.5	−0.04	22.3
1831–1223	6.92	12.60	30.97	5.3	−0.12	34.3
1831–1329	7.06	12.41	31.08	6.4	−0.21	20.9
1832–0644	5.50	12.73	33.56	9.0	0.16	52.7
1833–0559	5.79	12.39	33.63	5.8	0.13	18.5
1833–1055	7.28	11.77	31.91	8.4	−0.17	36.0
1834–0602	6.63	11.98	32.79	6.5	0.11	33.4
1835–0924	5.80	12.64	33.11	6.3	−0.09	20.6
1835–1020	5.91	12.13	33.92	2.6	−0.06	13.0
1837–0559	5.98	11.92	34.20	5.0	0.03	11.5
1837–0604	4.53	12.32	36.30	6.2	0.03	28.1
1837–1243	5.91	12.92	32.34	8.1	−0.35	11.2
1838–0453	4.72	12.83	34.92	8.2	0.10	22.2
1838–1046	6.80	12.29	31.83	4.3	−0.16	9.2
1839–0321	5.48	12.24	34.56	6.9	0.13	12.9
1839–0402	6.03	12.31	33.32	4.6	0.06	4.4
1839–0459	6.45	12.15	32.81	4.5	0.03	6.1
1839–06273	7.77	11.41	31.66	2.4	−0.01	1.7
1839–0643	6.29	12.11	33.20	6.5	−0.04	57.0
1841–0348	4.75	12.54	35.43	4.2	0.03	25.4
1842–0153	6.40	12.43	32.36	6.3	0.12	22.2
1842–0415	5.58	12.54	33.77	4.0	0.01	5.8
1843–0050	7.70	11.65	31.32	7.8	0.18	14.6
1843–0355	6.30	11.57	34.26	8.8	0.01	62.0
1843–0459	7.15	11.91	31.89	6.3	−0.05	67.9
1844–0310	5.91	12.37	33.45	8.9	0.01	52.3
1847–0438	6.14	12.51	32.69	4.8	−0.10	11.1
1847–0605	6.42	12.28	32.59	4.5	−0.15	15.8
1849+0127	5.49	12.60	33.84	4.7	0.08	10.2
1849–0317	5.68	12.59	33.46	1.8	−0.04	2.1
1850+0026	7.68	11.80	31.04	4.2	0.03	18.2
1852+0305	>7.48	< 11.99	<31.07	6.7	0.14	35.9
1853+0056	5.31	12.39	34.60	3.9	−0.00	3.2

Table 4. – *continued*

PSR J	$\log[\tau_c \text{ (yr)}]$	$\log[B_s \text{ (G)}]$	$\log[\dot{E} \text{ (erg s}^{-1}\text{)}]$	d (kpc)	z (kpc)	Luminosity (mJy kpc 2)
1855+0422	7.46	12.10	30.89	9.9	0.18	44.1
1856+0404	>7.82	<11.32	<31.73	7.0	0.09	23.5
1857+0210	5.85	12.48	33.34	15.4	-0.10	71.1
1858+0215	6.41	12.27	32.64	12.4	-0.11	33.8
1900+0227	6.02	12.17	33.63	4.2	-0.07	5.8
1901+0413	5.51	13.28	32.45	7.1	-0.03	54.9
1904+0412	9.43	10.05	31.04	4.0	-0.07	3.7
1905+0616	5.06	13.07	33.74	5.4	-0.02	11.7
1906+0912	7.97	11.51	31.04	5.5	0.09	9.7
1907+0740	7.13	11.80	32.15	6.8	-0.01	19.0
1907+0534	6.76	12.28	31.92	12.0	-0.21	51.8
1908+0909	5.18	12.54	34.56	8.8	0.08	17.0
1908+0839	6.09	11.83	34.18	9.6	0.04	45.2
1909+0912	4.99	12.46	35.11	8.2	0.04	23.5
1909+0616	5.76	12.60	33.28	8.5	-0.18	23.8
1910+0534	6.57	11.98	32.91	15.5	-0.45	98.5
1913+1145	5.99	12.10	33.84	14.7	0.12	92.9
1913+1011	5.23	11.55	36.46	4.5	-0.01	10.1
1913+0832	5.67	11.90	34.87	7.8	-0.12	37.7
1920+1110	7.71	11.45	31.66	5.0	-0.10	9.8